



Original

Anatomy and nomenclature of tree shrew lymphoid tissues

Nan SHI^{1,2)*}, Wei XIA^{1,2)*}, Ketong JI^{1,2)}, Yiwei FENG^{1,2)}, Hua LI^{1,2)}, Guangyao HE^{1,2)} and Anzhou TANG^{1,2)}

¹⁾Department of Otorhinolaryngology Head and Neck Surgery, The First Affiliated Hospital of Guangxi Medical University, No. 6, Shuangyong Street, Nanning 530021, P.R. China

²⁾Key Laboratory of Early Prevention and Treatment for Regional High Frequency Tumor (Guangxi Medical University), Ministry of Education, No. 22, Shuangyong Street, Nanning 530021, P.R. China

Abstract: The immune response plays a key role in the disease development of the organism, while immune function serves as an important indicator for animal models evaluation. The tree shrew (*Tupaia belangeri chinensis*), as a new laboratory animal with a close genetic relationship with primates, has been used to construct various disease models. However, the immune system of tree shrews, especially anatomical descriptions of lymph nodes, is still relatively unknown. In this study, a total of 16 different lymph nodes were identified, including superficial lymph nodes and deep lymph nodes. Superficial lymph nodes were located in the head and neck region (submandibular lymph node, parotid lymph node, deep and superficial cervical lymph nodes) and at the forelimb (axillary and accessory axillary lymph nodes, subscapular lymph node) and hindlimb (popliteal, sciatic, and inguinal lymph nodes). Deep lymph nodes comprise mediastinal lymph nodes located in thoracic cavity and abdominal lymph nodes that are mainly located in each mesentery (mesenteric, gastric, pancreatic-duodenal, renal lymph nodes) or along the major vessels (iliac lymph nodes). In addition, we described the spleen and thymus of the tree shrew, as well as two lymphoid tissues in the top wall of the nasal cavity and the oropharynx. This study mainly describes the tree shrew immune system from an anatomical and histopathological perspective and provides fundamental research references for the establishment of various animal models of tree shrews.

Key words: immune system, lymph nodes, *Tupaia belangeri*

Introduction

The tree shrew (*Tupaia belangeri chinensis*), as a small laboratory animal, shows a closer genetic relationship with primates than rats and mice [1]. For this reason, various tree shrew models of human diseases have been established, especially those for studying viral infections and immune processes such as human hepatitis B virus [2, 3], hepatitis C virus [4, 5], influenza virus [6, 7], herpes simplex virus (HSV) [8], Epstein-Barr virus (EBV) [9], and SARS-CoV-2 [10]. Immunological processes of the tree shrew correlate strongly with the oc-

currence and development of diseases [11]. The functions of immune-related genes and proteins, the role of immune cells, and the histopathological changes of immune tissues and organs should be systematically for revealing the immune response about diseases comprehensively and then effectively implement prevention and treatment. Previous studies showed the relatively similar immune system of tree shrews to humans. For example, the major histocompatibility complex (MHC), the important molecules of the immune response, and the genes encoding antibodies of tree shrew are highly homologous to those of humans [1, 12], as well as the differential

(Received 17 August 2021 / Accepted 26 October 2021 / Published online in J-STAGE 1 December 2021)

*These authors contributed equally to this work.

Corresponding author: A. Tang. email: anzhoutang@126.com

Supplementary Table: refer to J-STAGE: <https://www.jstage.jst.go.jp/browse/expanim>



This is an open-access article distributed under the terms of the Creative Commons Attribution Non-Commercial No Derivatives (by-nc-nd) License <<http://creativecommons.org/licenses/by-nc-nd/4.0/>>.

©2022 Japanese Association for Laboratory Animal Science

count of peripheral blood cells of tree shrew, compared with mice and rats, is also closer to that of humans [13]. These studies provide molecular and biological insights into the research on the immune system of tree shrews. However, no anatomical study about the organs of the immune system of tree shrew has been reported yet. The immune organs are important parts of the immune system, where immune cells generate, differentiate and mature and T- and B-lymphocytes settle and proliferate. It is also the main site of the immune response. Lymph nodes are important immune organs mainly to collect and filter lymphatic fluid from all over the body [14, 15]. Given that the invasion of pathogenic microorganisms or inflammation often causes tumefaction of local lymph nodes and other changes, the examination of lymph nodes can aid in understanding the immune response of the organism to a certain extent. To advance the immunological study of tree shrews, this paper outlined the distribution of immune organs including lymph nodes, spleen and thymus from the perspective of anatomy and histomorphology.

Materials and Methods

Animals

Experiments consisted of ten healthy adult tree shrews (6 males and 4 females; weight 130–150 g) that were purchased from the Kunming Institute of Zoology, Chinese Academy of Sciences. Before the experiments, tree shrews were individually housed in hanging metal cages (cage size 40 cm × 30 cm × 35 cm, resting box 15 cm × 12 cm × 12 cm). Housing conditions were as follows: the temperature was 23–25°C, the relative humidity was 40–60%, the photoperiod/dark duration was 12 h, and environmental noise did not exceed 60 dB. The animal experiments in this study were approved by the Animal Ethics Committee, Guangxi Medical University (approval number: 202105002). During the experiment, animal welfare was improved as much as possible, and humanitarian care was given during the euthanasia process.

Identification and dissection of lymph nodes

Before the experiments, tree shrews were euthanized by intraperitoneally injecting pentobarbital sodium at a dose of 120 mg/kg. The distribution of lymph nodes in the whole body was observed by using methylene blue injection as the lymph node tracer. The tracer was prepared with 3% hydrogen peroxide and methylene blue dye and injected into the end of each toe skin of four limbs using a 1-ml syringe with a 30-G needle. Then, the skin on the dorsal side of the anterior and posterior

palms was carefully peeled off under a dissecting microscope to reveal the stained lymphatic vessels. A microinjection glass capillary needle (the outside diameter at the tip was 1 mm) was gently inserted into the lymphatic vessels to continue to inject the tracer to identify the lymph nodes connected to the vessels. The position of lymph nodes was recorded through a photograph and reconfirmed in the same position in another tree shrew without tracer injection. Since lymph node tracers were hard to reach at sites distant from the injection point, lymph nodes in the head and neck, thoracic and abdominal cavities were carefully searched and identified under a dissecting microscope. After dissection, the tissue was fixed in the 10% neutral formalin solution for fixation.

Identification and dissection of thymus, spleen and tonsils

While searching for the lymph nodes in the thoracic and abdominal cavities of tree shrews, the thymus and spleen were carefully separated and placed in 10% formalin neutral fixative (Solarbio, Beijing, China). The head of euthanized tree shrews were taken to remove the external tissues, including skin, mandible, brain tissue, eyes and muscles. Then the rest parts were fixed in 10% neutral formalin for 48 h, and then decalcified in 10% EDTA decalcifying solution (Solarbio) for two weeks. When the decalcification was completed, head samples were serially separate along a coronal plane (0.5 cm thickness).

Histomorphology

All the separated tissues were dehydrated and embedded in paraffin sections, and 4 μm sections were cut with a microtome (RM2245, Leica, Wetzlar, Germany). All tissue sections were stained with an HE staining kit (Solarbio), and were examined with an optical microscope (BX53F, Olympus, Tokyo, Japan) linked to a digital camera (DP73, Olympus).

Immunohistochemical analysis

Lymphoid follicle tissue sections of tree shrews were immunohistochemically stained using an immunohistochemistry kit (SP-9000, ZSGB-Bio, Beijing, China). CD3 rabbit polyclonal (GB11014, Servicebio, Wuhan, China) and CD20 rabbit polyclonal antibodies (GB11540, Servicebio) were used as the primary antibodies at a dilution of 1/200 for 1 h at 37°C. Biotin conjugated goat anti-rabbit IgG was used as the secondary antibody. Diaminobenzidine (DAB) was used as the chromogen. The section was then counterstained with hematoxylin. Antigen retrieval was heat mediated with sodium citrate buffer (pH 6.0).

Results

Anatomical locations and histological structures of lymph nodes in the tree shrew

According to the anatomical and histomorphological verification, the tree shrew contains a total of 16 lymph nodes, which were divided into peripheral lymph nodes (head and neck, forelimbs and hindlimbs) and deep lymph nodes (intrathoracic and intra-abdominal lymph nodes) based on their locations. Table 1 describes the nomenclature of lymph nodes based on their locations and specific anatomical positions. Figure 1 shows a schematic diagram of lymph node locations of the tree shrew, including 10 pairs of bilateral lymph nodes, comprising all lymph nodes in the head and neck (submandibular lymph nodes, parotid lymph nodes, deep and superficial cervical lymph nodes), forelimbs (axillary and accessory axillary lymph nodes, subscapular axillary lymph nodes) and hindlimbs (popliteal, sciatic, and inguinal lymph nodes). The lymph nodes in the thoracic cavity are mainly located in the mediastinum, and were classified as mediastinal lymph nodes. Intra-abdominal lymph nodes are mainly located at each mesentery or along major vessels. The former includes mesenteric, gastric, pancreatic-duodenal lymph nodes, and the latter mainly refers to iliac lymph nodes on both sides of the abdom-

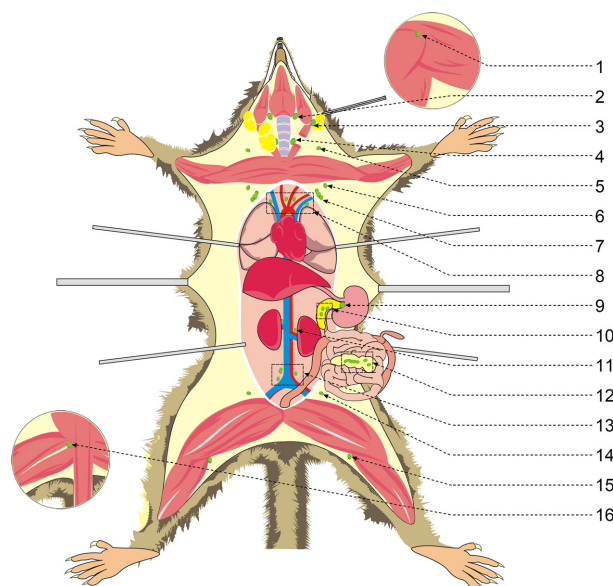


Fig. 1. Schematic diagram of lymph nodes in the tree shrew. (1) Subscapular lymph nodes; (2) Submandibular lymph nodes; (3) Parotid lymph nodes; (4) Cervical deep lymph nodes; (5) Cervical superficial lymph nodes; (6) Accessory axillary lymph nodes; (7) Axillary lymph nodes; (8) Mediastinal lymph nodes; (9) Gastric lymph nodes; (10) Pancreaticoduodenal lymph nodes; (11) Renal lymph nodes; (12) Mesenteric lymph nodes; (13) Iliac lymph node; (14) Inguinal lymph nodes; (15) Popliteal lymph nodes; (16) Sciatic lymph nodes.

Table 1. Nomenclature of lymph nodes based on their locations and the specific anatomical locations

No.	Name	Size	Shape	Position
Head and neck				
1	Submandibular lymph node	3–5	Ellipsoid	In sublingual gland near the cephalic side
2	Parotid lymph node	2–4	Ellipsoid	In deep parotid gland at the intersection with the edge of the occlusal muscle
3	Cervical superficial lymph node	3–4	Oval	Sternocleidomastoid muscle, lateral to the beginning of the clavicle, at the angle between the external jugular vein and the clavicle
4	Cervical deep lymph node	2–4	Oval	Deep sternocleidomastoid muscle, both sides of the trachea
Forelimb				
5	Axillary lymph node	2–3	Oval	Between the axillary artery and the ventral aspect of the latissimus dorsi muscle
6	Accessory axillary lymph node	2–3	Circle	Posterior border of the triceps brachii muscle and the border of the latissimus dorsi muscle
7	Subscapular lymph node	2–3	Circle	The surface of the triceps near the outer edge of the scapula
Hindlimb				
8	Inguinal lymph node	2–5	Oval	In the inguinal region immediately below the skin
9	Sciatic lymph node	4–5	Oval	Below the superficial gluteus muscle and above the sciatic nerve near the spinal side
10	Popliteal lymph node	2–5	Oval	Within the popliteal fossa on the head side of the gastrocnemius
Thoracic cavity				
11	Mediastinal lymph node	3–5	Circle	Near the aortic arch
Abdominal cavity				
12	Mesenteric lymph node	10–15	Ellipsoid	Near the aortic arch root of mesentery, the rest scatters in the wall of jejunum, ileum, and colon on the mesentery
13	Gastric lymph node	2–3	Circle	In the mesentery of the lesser curvature of the stomach
14	Pancreaticoduodenal lymph node	1–2	Circle	At the lesser curvature of the stomach mesentery of duodenum surrounded by pancreatic tissue
15	Renal lymph node	1–2	Circle	Renal hilum near the lower renal vessels
16	Iliac lymph node	3–1	Long oval	Para-aortic, bifurcation of iliac vessels

inal aorta. Figure 2 illustrates the anatomical location of lymph nodes and the surrounding structure: (1) Submandibular lymph node: Each side contains one lymph node, approximately 3–5 mm in size, located near the head of the sublingual gland in the superficial subcutaneous layer. Sometimes it is necessary to search for these lymph nodes on the inner side because they may be located inferior to the sublingual gland. (2) Parotid lymph node: It is located on the inner surface of the parotid glands on both sides, often on the surface of the masseter muscle. one on each side, approximately 2–4 mm in size, smaller than the submandibular lymph node. (3) Cervical

superficial lymph node: There are 1–2 on each side, approximately 3–4 mm in size. It is in the fat layer outside the clavicle end of the stern cephalic muscle, inside the external jugular vein, and above the clavicle. Fat separation and identification are needed to distinguish it. (4) Cervical deep lymph node: It is in the deep part of the neck and can be found in the gap between both sides of the trachea and the sternocephalic muscle. There were 1–2 lymph nodes on each side, approximately 2–4 mm in size. The superficial lymph nodes of the head and neck are commonly used as donor sites to treat lymphedema due to their large numbers and subcutaneous location

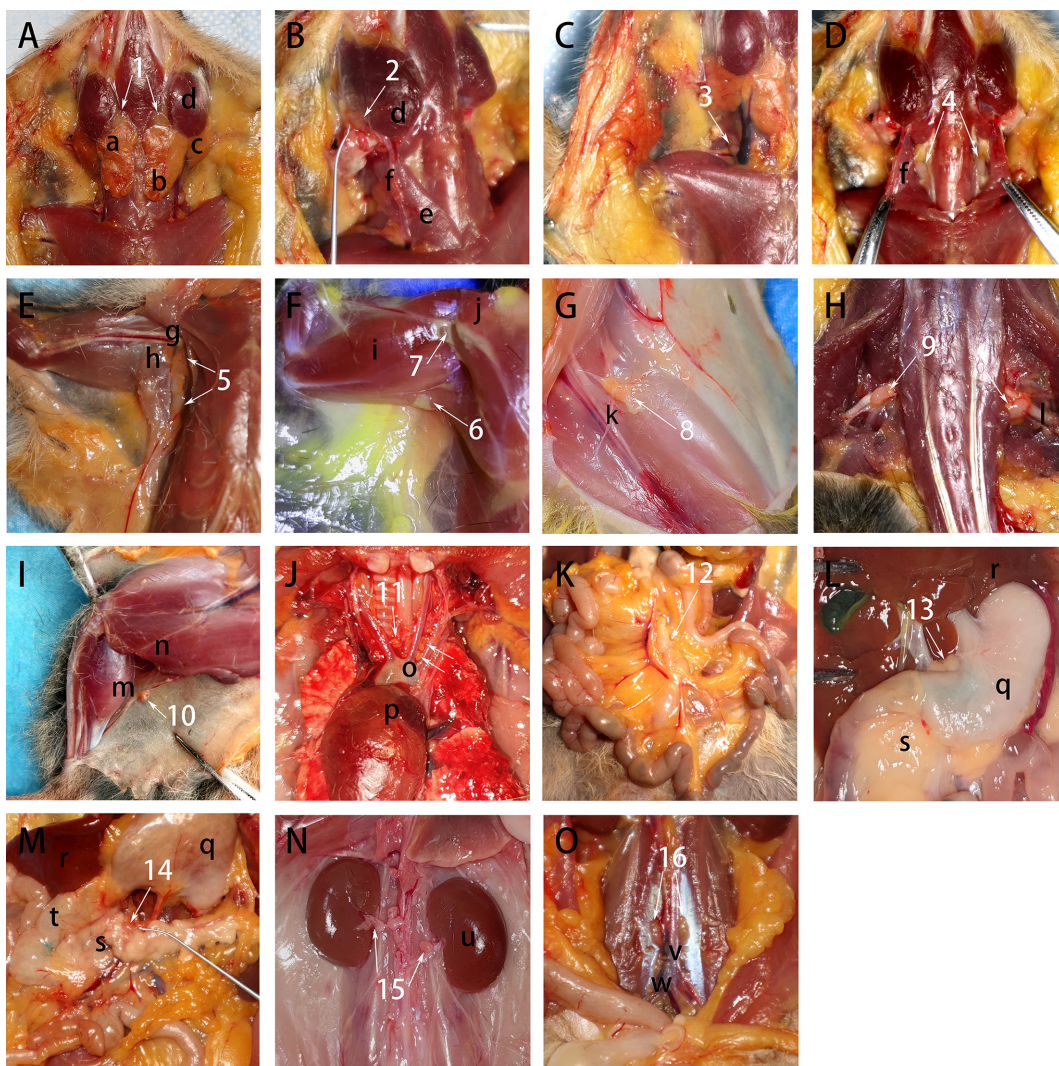


Fig. 2. Anatomical locations of lymph nodes in tree shrews. (ABCD) Ventral view of head and neck, including sublingual gland (a), submandibular gland (b), parotid gland (c), muscles of mastication (d), sternocleidomastoid muscle (e), external jugular vein (f); (E) ventral view of axillary region, including axillary vessels (g), latissimus dorsal muscular (h); (F) dorsal view of forelimb side, including brachial triceps (i), trapezius muscle (j); (G) view of inguinal region, including femoral vein (k); (H) dorsal view of sacral region, including sciatic nerve (k); (I) ventral view of hind limbs, including gastrocnemius (m), popliteal fossa (n); (J) medial view of thoracic cavity, including heart (p), aortic arch (o); (K) exposure of mesentery; (LMN) intra-abdominal view, including liver (r), stomach (q), duodenum (t), pancreas (s), kidney (u); (O) intra-abdominal view with the viscera set aside, including the abdominal vein (v), and iliac vessels (w). Numbers 1–16 are described in Table 1.

[16–18]. (5) Axillary lymph node: This is a group of larger lymph nodes. Each side often consists of 2–4 lymph nodes, approximately 2–3 mm in size, often arranged in rows along the long axis of the trunk. These were located between the axillary artery and vein roots, along the ventral side of the latissimus dorsi muscle. It is easy to identify after separating the chest muscles in front of the trunk. There were more lymph nodes in this location than in other positions, which often drain most of the upper limbs and chest wall lymph fluid. It is a common sentinel lymph node for breast cancer metastasis [19]. Due of its fixed location, it is easy to find and isolate, which shows its potential as an animal model for tumor lymph node metastasis. (6) Accessory axillary lymph node: Located at the junction of the posterior edge of the triceps brachii muscle and the edge of the latissimus dorsi, one on each side, size 2–3 mm. (7) Subscapular lymph node: Located at the junction of the triceps brachii surface and the scapula, usually one on each side, 2–3 mm in size. (8) Inguinal lymph node: Usually, one on each side, 2–5 mm in size, located in the lateral abdominal fold of the groin area, close to the subcutaneous, easy to peel off and lose with the skin when separated. Due of its superficial position, it has become the main site of injection treatment called the lymphatic drug delivery system (LDDS) [20]. (9) Sciatic lymph node: It is located on the ventral side of the superficial gluteus muscle, on the side of the sciatic tuberosity, and above the sciatic nerve near the spine, one on each side, and the size is approximately 4–5 mm. (10) Popliteal lymph node: Located in the popliteal fossa on the cephalic surface of the gastrocnemius muscle, one on each side, approximately 2–5 mm in size. (11) Mediastinal lymph node: It is in the anterior side of the aortic arch, usually close to the root of the great vessels. There are 3–4 lymph nodes, approximately 3–5 mm in size. (12) Mesenteric lymph node: This is a group of lymph nodes located at the root of the mesentery. It is formed by a fusion of 5–7 lymph nodes each about 10–15 mm in diameter. Some smaller lymph nodes can be seen scattered on the mesentery and intestinal wall. (13) Gastric lymph node: There were 1–2 lymph nodes located in the lesser curvature of the stomach, 2–3 mm diameter. (14) Pancreaticoduodenal lymph node: It is above the mesentery of the twelfth finger, and it is surrounded by pancreatic tissue, including a lymph node, 1–2 mm in size. (15) Renal lymph node: Usually, one on each side, 1–2 mm in size, located below the renal blood vessels near the renal hilum. (16) Iliac lymph node: Located on either side of the distal end of the abdominal aorta, near the bifurcation of the iliac vessels, it is usually long oval and 1–3 mm in size. (The number of lymph

nodes in the tree shrew is arranged in the attachment Supplementary Table 1).

After being injected into the skin of the four limbs, hydrogen peroxide produces tiny bubbles that inflate the lymphatic vessels. It leads to the dye tracer being absorbed into the lymphatic vessels, which are stained blue. After dye injection, the lymphatic vessels could be observed on the dorsal and palmar sides of the foot, appearing as a honeycomb grid (Fig. 3A). Although the dye is occasionally absorbed by the veins, the lymphatic vessels can be distinguished from the dyed veins since the diameter of the veins are slightly larger than that of the lymphatic vessels (Fig. 3B). Although both vein and lymphatic vessels had valves where the dye could be seen to accumulate, they could be distinguished by observing blood retained in most veins. Three types of lymph nodes were identified in the four limbs after the dye entered the lymphatic vessels upon delivery with microinjection glass capillary needles (Fig. 3). The dorsal palmar lymphatic network of the upper limbs was observed to converge into a single lymphatic vessel that traveled around the stem of the forearm and up the lateral side of the upper limbs to the dorsum, where it converged into the subscapular lymph nodes (Fig. 3C). The dorsal lymphatic vessels of the foot traveled laterally to the ankle, up along the midline of the gastrocnemius muscle, through the popliteal lymph nodes and into the gluteal muscle gap. Then, they traveled along the femoral vessels into the sciatic lymph nodes (Fig. 3D).

The histological structure of all lymph nodes and tissues identified in this paper was confirmed using pathological sections (Fig. 4). Most of the tree shrew lymph nodes presented a clear histological structure, and the envelope was composed of denser connective tissue. The parenchyma comprised the cortex and medulla. Lymph follicle could be seen in the cortical area. The germinal center structures were apparent, resembling those of human lymph nodes. Only a few lymph nodes showed blurred histological structures and unclear boundaries of the cortex and renal medulla, which sometimes were difficult to distinguish.

Anatomical locations and histological structures of thymus, spleen, and tonsils in the tree shrew

Immune organs refer to those organs that performs immune functions, and consist mostly of lymphoid tissues. Generally, they are divided into central immunological organs (thymus, bone marrow) and peripheral immune organs (lymph nodes, spleen, tonsils). The thymus of tree shrews was located above the heart, behind the breastbone and in front of the major vessels of the mediastinum (Fig. 5), with a yellowish appearance

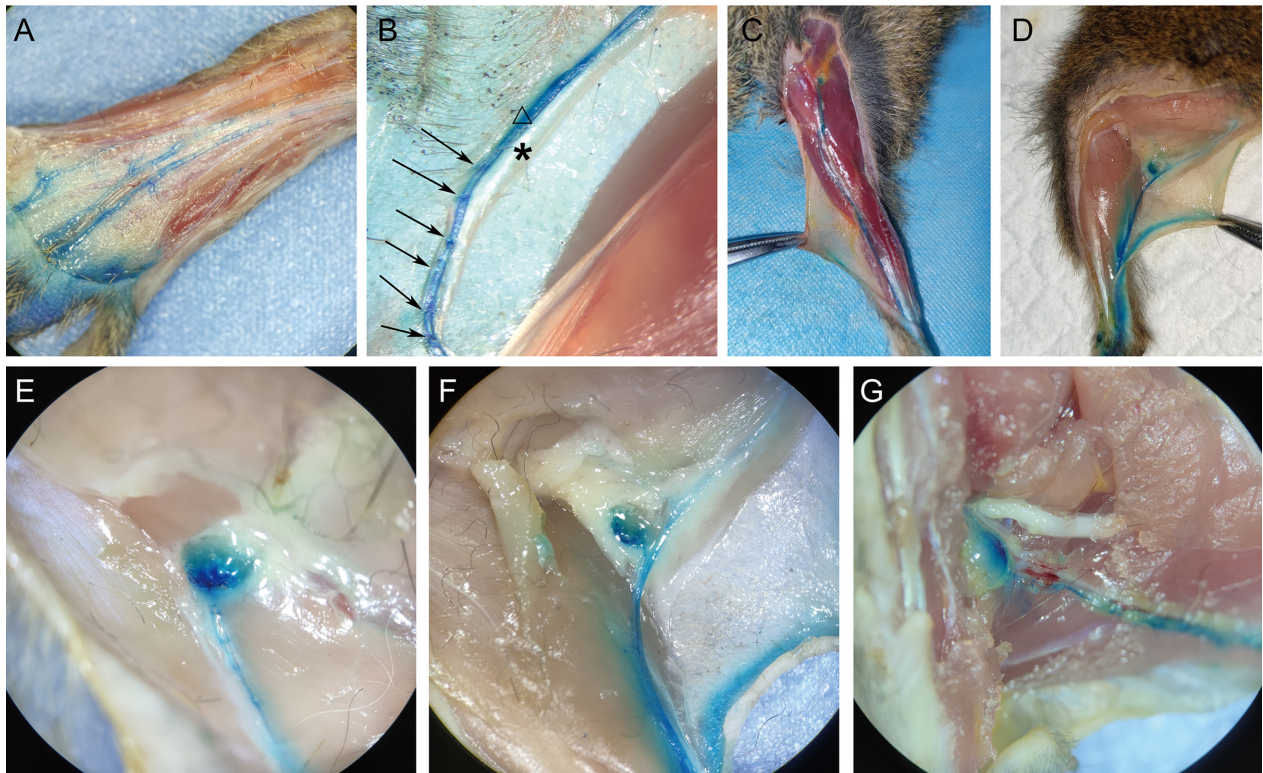


Fig. 3. Lymphatic tracer identification in four limbs. (A) Dorsal lymphatic network of the tree shrew hind limbs appearing as a honeycomb grid; (B) bead-like valves, visible in the blue-stained lymphatic vessel (Δ), accompanying the saphenous vein (*) in the hind limbs. (CD) Lymphatic vessels travel in the fore and hind limbs. (EFG) The tracer shows lymph nodes; subscapular lymph nodes, popliteal lymph nodes and sciatic lymph nodes are shown.

and oval-shaped lamellae, and was encapsulated in adipose tissue (Fig. 5). The thymus of the tree shrew was composed of the peritoneum, cortex and medulla. The cortex was thin, while the medulla was thick, indistinctly demarcated and crossed (Fig. 5). All samples were found to have obvious thymus corpuscles, similar to those of humans in structure. It may suggest a similar function of the thymus between tree shrews and humans.

The spleen was long and brownish red, located in the deep abdominal cavity, adjacent to the stomach and duodenum, with a length of approximately 1.5–2 cm and a brittle and soft texture. No accessory spleen was found (Fig. 5). The tree shrew spleen was covered by a peritoneum composed of dense connective tissue, which penetrated deep into the parenchyma to form trabeculae. The parenchyma had cross-distributed red and white pulps and many lymph follicles with a clear structure, showing no significantly different histological features from those of humans (Fig. 5).

In the head section, clustered lymphoid tissue was found in the parietal wall of the posterior nasal cavity and the two walls of the terminal oropharyngeal segment of the tree shrew (Fig. 6), resembled the structure of human palatine tonsils and pharyngeal tonsils. The base of the palatine tonsils was close to the sphenoid bone,

and covered with pseudostratified ciliated columnar epithelium. The parenchyma consisted of lymphocytes with few lymph follicles observed. The pharynx tonsils were located on both sides of the lateral wall of the oropharynx and protruded towards the oral cavity, with an intact peritoneum and 1–2 lymph follicles (Fig. 6).

Through immunohistochemical staining, the cell composition in the lymph nodes of tree shrews (Fig. 7) could be found: CD3 staining could mark T lymphocytes, which were mainly scattered in the mantle and marginal areas of lymphoid follicles; B cells expressing CD20 were mainly distributed in the germinal center, and clusters or single B cells existed in the red pulp.

Discussion

This study initially investigated the distribution of lymph nodes in tree shrews and their histological composition and demonstrated the anatomical location and histomorphological characteristics of the main immune organs. The anatomical atlas of the lymphatic system of tree shrews has not been reported in previous literature. We identified a total of 16 lymph nodes of tree shrews through dissection. The nomenclature was based on the lymphatic anatomical location of each lymph node and

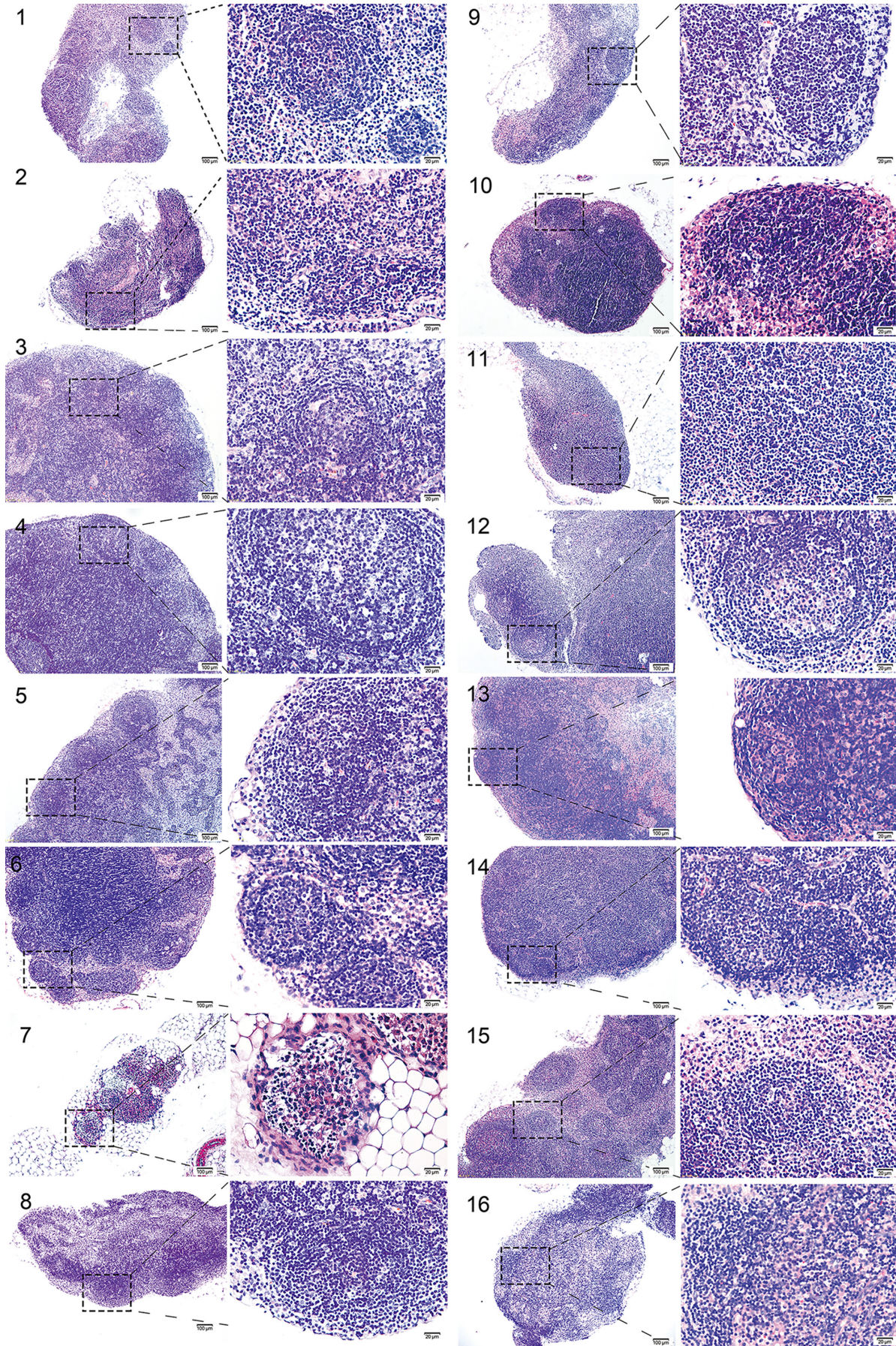


Fig. 4. A light micrograph of the lymph nodes of tree shrews stained with HE (100× and 400×). Numbers 1–16 have been described in Table 1.

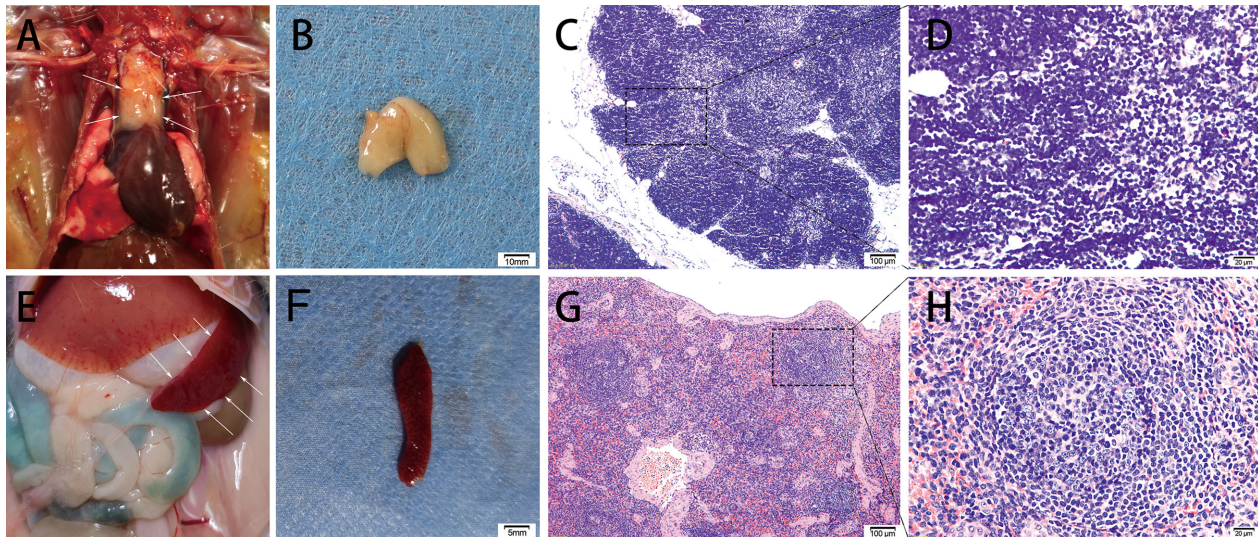


Fig. 5. General anatomical structure and histological structure of the thymus and spleen of tree shrews. (ABEF) Anatomical structures and adjoining of tree shrew thymus and spleen; (CDGH) HE staining of thymus and spleen (100× and 400×).

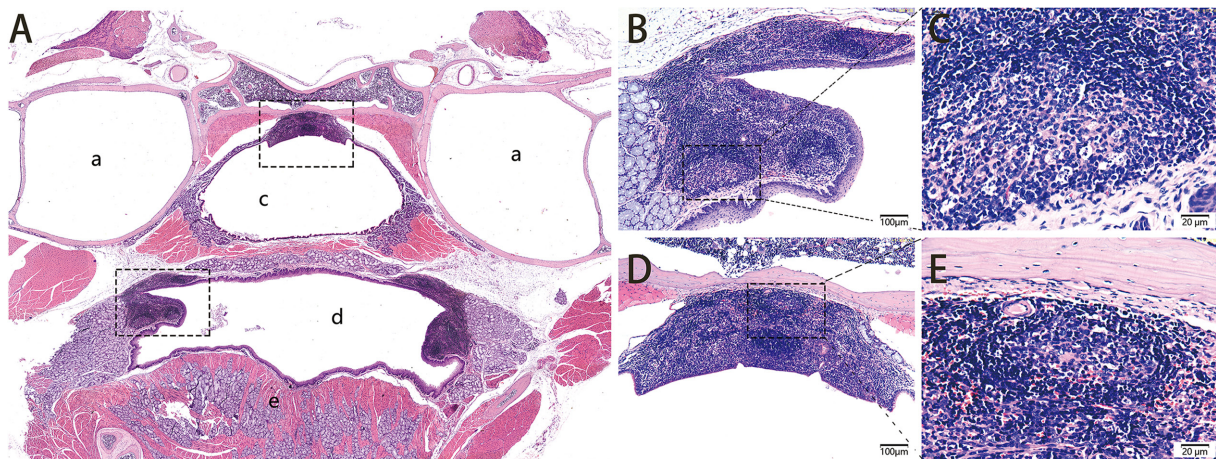


Fig. 6. Histological structure of the tree shrew tonsils. (A) Coronal plane of the tree shrew head, including listening bubbles (a), sphenoid bone (b), posterior nasal cavity (c), oral cavity (d), and tongue (e). (BCDE) HE staining of palatine tonsils and pharyngeal tonsils (100× and 400×).

its adjacency, with reference to the naming of lymph nodes in experimental mice [21–23]. Most of the locations and nomenclature were consistent with those of experimental mice. Unlike the experimental mice, a type of lymph node was found in the scapular region of the tree shrew, through which the lymphatic vessels draining the forelimbs passed. Their locations were superficial and constant, distant from the axillary lymph node group and the accessory axillary lymph node in the axillary region. Therefore, those two types of lymph nodes were not totally the same as the common functional subdivision. Specifically, this lymph node in the tree shrew was equivalent to the subscapular lymph nodes of humans and was considered one of the sentinel lymph nodes of breast cancer metastasis [24]. In addition, this study found that tree shrews had a pair of tissues with lympho-

cyte aggregates in the lateral wall of the oropharynx and in the parietal wall of the nasopharynx. The latter, with lymph follicles inside, was considered similar to the human pharyngeal tonsils which was not found in rats [25]. The human pharynx is rich in lymphoid tissue. The large lymphoid masses are arranged in a pharyngeal lymphatic ring (Waldeyer lymphatic ring) [26]. The inner ring consists mainly of the tonsilla pharyngea (adenoids) above, the palatine tonsils on both sides, the lingual tonsils below, and the lymphoid follicles in the retropharyngeal wall. The inner ring of lymph nodes flows to the cervical lymph nodes, which are interconnected to form an outer ring. Since the inner ring is in relatively close and frequent contact with the external environment, the Waldeyer lymphatic ring plays the leading role in confronting the invasion of inhaled or in-

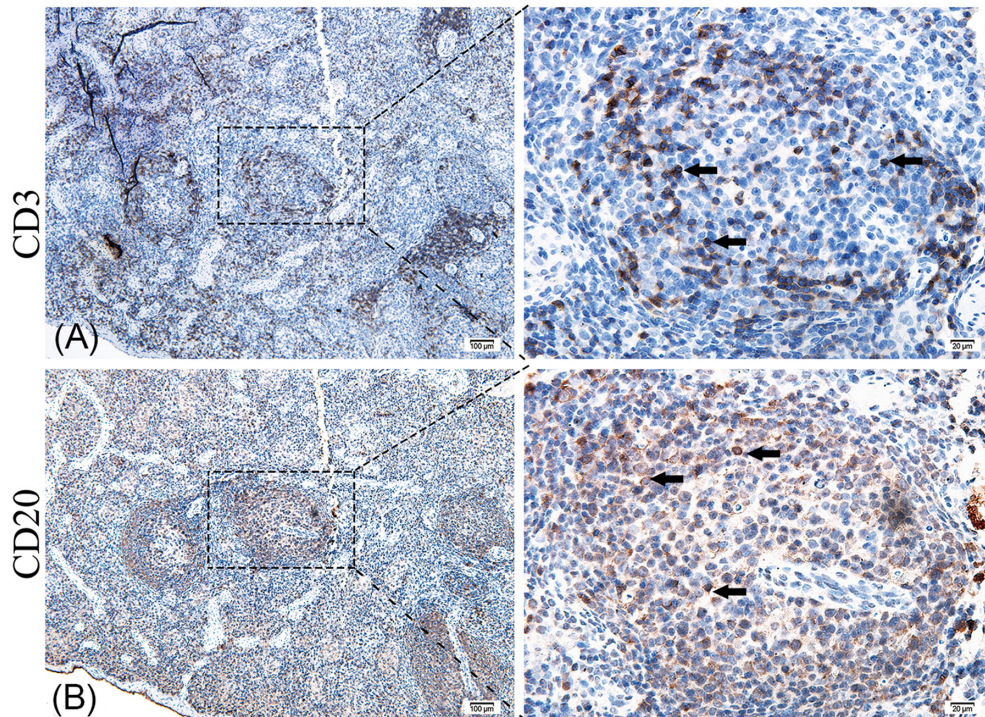


Fig. 7. Immunohistochemistry of lymphoid follicles in tree shrew (100× and 400×). (A) CD3 rabbit polyclonal positive cells (arrowheads). (B) CD20 rabbit polyclonal positive cells (arrowheads).

gested pathogens. Therefore, it is considered the first line of defense against external infection and is an essential component of the lymphatic system [27]. It suggests that tree shrews may have an advantage in immune tissue distribution compared to the rodents.

Visualization of lymphatic vessels has been a difficult task in lymphatic system anatomy. Earlier studies identified lymphatic vessels by injecting mercury into the skin of living animals [28–30], which had faded away due to toxicity. Dye injections have emerged as alternatives to mercury injections and are still commonly used. Current methods for lymphatic vessel visualization are mainly the blue dye method and radionuclide tracer technique. This study used a modified dye method developed by Suami *et al.* [31], combined with using hydrogen peroxide to identify lymphatic vessels that produce microbubbles after injection. The subsequent inflation of fine lymphatic vessels and lumen expansion help to improve the success rate of microinjection needle insertion into lymphatic vessels. By injecting the dye into the subcutaneous interstitial tissue, the capillary lymphatic vessels of injection sites could absorb the dye into the lymphatic system, thus causing the colorless lymphatic vessels and lymph nodes to show blue color and facilitating observation. Since it existed in a dissolved state, methylene blue dye easily entered the lymphatic vessels and the capillaries after injection. Extensive staining of the interstitial tissue space with a large

injection dose easily occurred. The solution migrated fast, making it difficult to track the lymphatic vessel travel to identify the lymphatic vessels that entered the thoracic and abdominal cavities. Suami *et al.* [32] used an injection mixing lead tetroxide at 40°C to replace the dye and injected it into the lymphatic vessels. Lead tetroxide is insoluble in hot milk to create a colloidal suspension. The solid lead tetroxide powder prevented rapid migration in the lumen compared to the dye. However, the lead tetroxide solution cannot be maintained at a constant temperature (40°C) during the operation. The lead tetroxide will separate from the water and aggregate into large solid particles when the solution's temperature decreases to room temperature. This solution does not easily enter the fine lymphatic vessels and even blocks the lymphatic vessels and microinjection needle, making the operation more difficult.

Since tree shrews have been proposed as experimental animals, many studies on tree shrews have been reported. However, most of the studies are applied research, such as the construction of tree shrew disease models, while much basic research has not been resolved. For example, tree shrew strains with a pure genetic background are still being established [33, 34]. Additionally, there are only few tree shrew immortalized cell lines available [35–37]. Unfortunately, some reagents for working with tree shrew are lack, such as tree shrew specific antibodies. Therefore, the primary research of

tree shrews is still fundamental and should focus on achievement transformation to broad application.

In short, we described the anatomy and histomorphology of the tree shrew's lymph nodes, spleen, thymus, and tonsils. We hope that our research can provide a reference for the related study of tree shrews immunology in the future.

Conflicts of Interest

The authors declare no competing financial interests.

Acknowledgments

We thank the members of our research groups for their discussions and comments on this study. We thank the Kunming zoology Institute, the Chinese Academy of Science for providing experiment animals and the Experimental Animal Center of Guangxi Medical University for feeding animals. This study was supported by the National Natural Science Foundation of China (Grant No. 81760189 and Grant No. 32060132), the Innovation Project of Guangxi Graduate Education (Grant No. YCBZ2020050) and the University Student Innovative Plan (202010598006).

References

- Fan Y, Huang ZY, Cao CC, Chen CS, Chen YX, Fan DD, et al. Genome of the Chinese tree shrew. *Nat Commun.* 2013; 4: 1426. [Medline] [CrossRef]
- Walter E, Keist R, Niederöst B, Pult I, Blum HE. Hepatitis B virus infection of tupaia hepatocytes in vitro and in vivo. *Hepatology.* 1996; 24: 1–5. [Medline]
- Wang FS. Current status and prospects of studies on human genetic alleles associated with hepatitis B virus infection. *World J Gastroenterol.* 2003; 9: 641–644. [Medline] [CrossRef]
- Tong Y, Zhu Y, Xia X, Liu Y, Feng Y, Hua X, et al. Tupaia CD81, SR-BI, claudin-1, and occludin support hepatitis C virus infection. *J Virol.* 2011; 85: 2793–2802. [Medline] [CrossRef]
- Zhao X, Tang ZY, Klumpp B, Wolff-Vorbeck G, Barth H, Levy S, et al. Primary hepatocytes of *Tupaia belangeri* as a potential model for hepatitis C virus infection. *J Clin Invest.* 2002; 109: 221–232. [Medline] [CrossRef]
- Li R, Yuan B, Xia X, Zhang S, Du Q, Yang C, et al. Tree shrew as a new animal model to study the pathogenesis of avian influenza (H9N2) virus infection. *Emerg Microbes Infect.* 2018; 7: 166. [Medline] [CrossRef]
- Sanada T, Yasui F, Honda T, Kayesh MEH, Takano JI, Shiogama Y, et al. Avian H5N1 influenza virus infection causes severe pneumonia in the Northern tree shrew (*Tupaia belangeri*). *Virology.* 2019; 529: 101–110. [Medline] [CrossRef]
- Li L, Li Z, Wang E, Yang R, Xiao Y, Han H, et al. Herpes simplex virus 1 infection of tree shrews differs from that of mice in the severity of acute infection and viral transcription in the peripheral nervous system. *J Virol.* 2015; 90: 790–804. [Medline] [CrossRef]
- Wang Z, Yi X, Du L, Wang H, Tang J, Wang M, et al. A study of Epstein-Barr virus infection in the Chinese tree shrew (*Tupaia belangeri chinensis*). *Virology.* 2017; 14: 193. [Medline] [CrossRef]
- Zhao Y, Wang J, Kuang D, Xu J, Yang M, Ma C, et al. Susceptibility of tree shrew to SARS-CoV-2 infection. *Sci Rep.* 2020; 10: 16007. [Medline] [CrossRef]
- Parkin J, Cohen B. An overview of the immune system. *Lancet.* 2001; 357: 1777–1789. [Medline] [CrossRef]
- Zhang J, Xiao H, Bi Y, Long Q, Gong Y, Dai J, et al. Characteristics of the tree shrew humoral immune system. *Mol Immunol.* 2020; 127: 175–185. [Medline] [CrossRef]
- Feng Y, Xia W, Ji K, Lai Y, Feng Q, Chen H, et al. Hemogram study of an artificially feeding tree shrew (*Tupaia belangeri chinensis*). *Exp Anim.* 2020; 69: 80–91. [Medline] [CrossRef]
- Bogoslowski A, Kubes P. Lymph nodes: the unrecognized barrier against pathogens. *ACS Infect Dis.* 2018; 4: 1158–1161. [Medline] [CrossRef]
- Willard-Mack CL. Normal structure, function, and histology of lymph nodes. *Toxicol Pathol.* 2006; 34: 409–424. [Medline] [CrossRef]
- Cheng MH, Huang JJ, Nguyen DH, Saint-Cyr M, Zenn MR, Tan BK, et al. A novel approach to the treatment of lower extremity lymphedema by transferring a vascularized submental lymph node flap to the ankle. *Gynecol Oncol.* 2012; 126: 93–98. [Medline] [CrossRef]
- Piyaman P, Patchanee K, Oonjitti T, Ratanalekha R, Yodrabum N. Surgical anatomy of vascularized submental lymph node flap: Sharing arterial supply of lymph nodes with the skin and topographic relationship with anterior belly of digastric muscle. *J Surg Oncol.* 2020; 121: 144–152. [Medline]
- Uygun S, Ozturk C, Bozkurt M, Kwiecien G, Madajka M, Simeonow M. A new vascularized cervical lymph node transplantation model: an anatomic study in rats. *Ann Plast Surg.* 2013; 71: 671–674. [Medline] [CrossRef]
- Viale G, Sonzogno A, Pruneri G, Maffini F, Masullo M, Dell'Orto P, et al. Histopathologic examination of axillary sentinel lymph nodes in breast carcinoma patients. *J Surg Oncol.* 2004; 85: 123–128. [Medline] [CrossRef]
- Kato S, Takeda K, Sukhbaatar A, Sakamoto M, Mori S, Shiga K, et al. Intranodal pressure of a metastatic lymph node reflects the response to lymphatic drug delivery system. *Cancer Sci.* 2020; 111: 4232–4241. [Medline] [CrossRef]
- Pasierbek M. Functional anatomy of the mediastinal lymph nodes in rats. *Lymphat Res Biol.* 2014; 12: 157–163. [Medline] [CrossRef]
- Sun R, Gao B, Guo CB. [Anatomy and histology characteristics of lymph node in nude mice]. *Beijing Da Xue Xue Bao.* 2017; 49: 893–898. (in Chinese) [Medline]
- Yu Y, Zhang B, Jin S. Study on the distribution of lymphatic system in mice. *Journal of Hangzhou Normal University (Natural Science Edition).* 1982; 103–107.
- Krzhevitsky PI, Kanaev SV, Novikov SN, Chernaya AV, Krivorotko PV, Semiglazov VF, et al. [Use of SPECT-CT for visualization of sentinel lymph nodes in breast cancer patients]. *Vopr Onkol.* 2015; 61: 624–628. (in Russian) [Medline]
- Koornstra PJ, de Jong FI, Vlek LF, Marres EH, van Breda Vriesman PJ. The Waldeyer ring equivalent in the rat. A model for analysis of oronasopharyngeal immune responses. *Acta Otolaryngol.* 1991; 111: 591–599. [Medline] [CrossRef]
- Masters KG, Zeff D, Lasrado S. *Anatomy, head and neck, tonsils.* Treasure Island: StatPearls; 2021.
- Bogaerts M, Deggoujif N, Huart C, Hupin C, Laureyns G, Lemkens P, et al. Physiology of the mouth and pharynx, Waldeyer's ring, taste and smell. *B-ENT.* 2012; 8:(Suppl 19): 13–20. [Medline]
- Cruikshank WC. *The anatomy of the absorbing vessels of the human body.* London: G. Nicol. 1786.
- Mascagni P. *Vasorum lymphaticorum corporis humani historia et ichonographia.* Sienne: P. Carli. 1787.

30. Sappey PC. Anatomie, physiologie, pathologie des vaisseaux lymphatiques. Paris: Adrien Delahaye; 1874.
31. Suami H, Taylor GI, Pan WR. A new radiographic cadaver injection technique for investigating the lymphatic system. *Plast Reconstr Surg.* 2005; 115: 2007–2013. [[Medline](#)] [[CrossRef](#)]
32. Suami H, Shin D, Chang DW. Mapping of lymphosomes in the canine forelimb: comparative anatomy between canines and humans. *Plast Reconstr Surg.* 2012; 129: 612–620. [[Medline](#)] [[CrossRef](#)]
33. Xiao J, Liu R, Chen CS. Tree shrew (*Tupaia belangeri*) as a novel laboratory disease animal model. *Zool Res.* 2017; 38: 127–137. [[Medline](#)]
34. Yao YG. Creating animal models, why not use the Chinese tree shrew (*Tupaia belangeri chinensis*)? *Zool Res.* 2017; 38: 118–126. [[Medline](#)]
35. Gu T, Yu D, Li Y, Xu L, Yao YL, Yao YG. Establishment and characterization of an immortalized renal cell line of the Chinese tree shrew (*Tupaia belangeri chinensis*). *Appl Microbiol Biotechnol.* 2019; 103: 2171–2180. [[Medline](#)] [[CrossRef](#)]
36. Yin B, Song Q, Chen L, Li X, Han Y, Wang X, et al. Establishment of an immortalized intestinal epithelial cell line from tree shrews by lentivirus-mediated hTERT gene transduction. *Cytotechnology.* 2019; 71: 107–116. [[Medline](#)] [[CrossRef](#)]
37. Zhang X, Yu D, Wu Y, Gu T, Ma N, Dong S, et al. Establishment and transcriptomic features of an immortalized hepatic cell line of the Chinese tree shrew. *Appl Microbiol Biotechnol.* 2020; 104: 8813–8823. [[Medline](#)] [[CrossRef](#)]